Burgess, R. R., & Jendrisak, J. J. (1975) *Biochemistry 14*, 4634.
Carpousis, A. J., & Gralla, J. D. (1980) *Biochemistry 19*, 3245.
Cashel, M. T., & Gallant, J. (1968) *J. Mol. Biol. 34*, 317.
Chamberlin, M. J. (1976) in *RNA Polymerase* (Losick, R., & Chamberlin, M., Eds.) p 17, Cold Spring Harbor Laboratory, Cold Spring Harbor, NY.
Chamberlin, M., & Berg, P. (1962) *Proc. Natl. Acad. Sci. U.S.A. 48*, 81.
Chamberlin, M., & Berg, P. (1964) *J. Mol. Biol. 8*, 708.
Chan, P. T., Ohmori, H., Tomizawa, J., & Lebowitz, J. (1985) *J. Biol. Chem. 260*, 8925.
Cowie, A., Jat, P., & Kamen, R. (1982) *J. Mol. Biol. 159*, 225.
Dahlberg, J. E., & Blattner, F. R. (1973) in *Virus Res., ICN–UCLA Symp. Mol. Biol., Proc., 2nd*, 533.
Darlix, J., & Horaist, M. (1976) *Nature (London) 256*, 288.
Dausse, J.-P., Sentenac, A., & Fromageot, P. (1975) *Eur. J. Biochem. 57*, 569.
Donis-Keller, H. (1980) *Nucleic Acids Res. 8*, 3133.
Donis-Keller, H., Maxam, A. M., & Gilbert, W. (1977) *Nucleic Acids Res. 4*, 2527.
Downey, K. M., & So, A. G. (1970) *Biochemistry 9*, 2520.
Dunn, J. J., & Studier, F. W. (1981) *J. Mol. Biol. 148*, 303.
Ebina, Y., & Nakazawa, A. (1983) *J. Biol. Chem. 258*, 7072.
Falaschi, A., Adler, J., & Khorana, H. G. (1963) *J. Biol. Chem. 238*, 3080.
Gilbert, W. (1976) in *RNA Polymerase* (Losick, R., & Chamberlin, M., Eds.) p 193, Cold Spring Harbor Laboratory, Cold Spring Harbor, NY.
Hansen, U. M., & McClure, W. R (1980) *J. Biol. Chem. 255*, 9564.
Kassavetis, G. A., & Chamberlin, M. J. (1981) *J. Biol. Chem. 256*, 2777.
Levine, A. D., & Rupp, W. D. (1978) in *Microbiology—1978* (Schlessinger, D., Ed.) p 163, American Society of Microbiology, Washington, D.C.
Lilley, D. M. J. (1980) *Proc. Natl. Acad. Sci. U.S.A. 77*, 6468.
Maizels, N. M. (1973) *Proc. Natl. Acad. Sci. U.S.A. 70*, 3585.
Maxam, A. M., & Gilbert, W. (1980) *Methods Enzymol. 65*, 499.
McClure, W. R. (1985) *Annu. Rev. Biochem. 54*, 171.
McClure, W. R., Cech, C. L., & Johnson, D. E. (1978) *J. Biol. Chem. 253*, 8941.
Minkley, E. G., & Pribnow, D. (1973) *J. Mol. Biol. 77*, 255.
Moses, V., & Sharp, P. B. (1972) *J. Gen. Microbiol. 71*, 181.
Munson, L. M., & Reznikoff, W. S. (1981) *Biochemistry 20*, 2081.
Nierman, W. C., & Chamberlin, M. J. (1979) *J. Biol. Chem. 254*, 7921.
Nishimura, S., Jacob, T. M., & Khorana, H. G. (1964) *Proc. Natl. Acad. Sci. U.S.A. 52*, 1494.
Paetkau, V., Coulter, M. B., Flintoff, W. G., & Morgan, A. R. (1972) *J. Mol. Biol. 71*, 293.
Parker, R. C. (1983a) *Gene 26*, 127.
Parker, R. C. (1983b) Ph.D. Dissertation, Yale University, New Haven, CT.
Patient, R. K. (1979) *Nucleic Acids Res. 6*, 2647.
Peattie, D. A. (1979) *Proc. Natl. Acad. Sci. U.S.A. 76*, 1760.
Reisbig, R., & Hearst, J. E. (1981) *Biochemistry 20*, 1907.
Swerdlow, H., & Guthrie, C. (1984) *J. Biol. Chem. 259*, 5197.
Tomizawa, J., & Itoh, T. (1981) *Proc. Natl. Acad. Sci. U.S.A. 78*, 6096.
Travers, A. A., & Burgess, R. R. (1969) *Nature (London) 222*, 537.
Walseth, T. F., & Johnson, R. A. (1979) *Biochim. Biophys. Acta 562*, 11.
Wurst, R. M., Vournakis, J. N., & Maxam, A. M. (1978) *Biochemistry 17*, 4493.

Site Specificity of Psoralen–DNA Interstrand Cross-Linking Determined by Nuclease *Bal*31 Digestion†

Wei-ping Zhen,‡ Ole Buchardt,§ Henrik Nielsen,‡ and Peter E. Nielsen*,‡

Department of Biochemistry B, The Panum Institute, University of Copenhagen, DK-2200 Copenhagen N, Denmark, and Chemical Laboratory II, The H. C. Ørsted Institute, University of Copenhagen, DK-2100 Copenhagen Ø, Denmark

Received April 29, 1986; Revised Manuscript Received July 7, 1986

ABSTRACT: A novel method for determination of psoralen photo-cross-linking sites in double-stranded DNA is described, which is based on a pronounced inhibition of *Bal*31 exonuclease activity by psoralen–DNA interstrand cross-links. The results using a 51 base pair fragment of plasmid pUC19 and a 346 base pair fragment of pBR322 show that 5′-TA sequences are preferred cross-linking sites compared to 3′-TA sequences. They also indicate that sequences flanking the 5′-TA site influence the cross-linking efficiency at the site. The DNA photo-cross-linking by 4,5′,8-trimethylpsoralen and 8-methoxypsoralen was analyzed, and these two psoralens showed identical site specificity. The 5′-TA preference is rationalized on the basis of the local DNA structure in terms of the π–π electronic interaction between the thymines and the intercalated psoralens, as well as on the base tilt angles of the DNA.

It is generally assumed that the light-induced formation of psoralen–DNA adducts, and especially DNA interstrand cross-links, is intimately associated with many of the photobiological effects exhibited by the psoralens [see Ben-Hur & Song (1984) for a review]. These adducts may also be highly relevant when discussing the beneficiary effects (plaque clearing) as well as the unwarranted side effects (e.g., skin phototoxicity and the suspected carcinogenicity) in the therapeutical applications of these compounds (Andersen &

† Supported by the Danish Natural Science Research Council. P.E.N. is a "Niels Bohr Fellow" through the Egmont Foundation.
* Correspondence should be addressed to this author.
‡ The Panum Institute, University of Copenhagen.
§ The H. C. Ørsted Institute, University of Copenhagen.

0006-2960/86/0425-6598$01.50/0

Voorhees, 1980). Furthermore, psoralens have successfully been used as probes in the study of the structure of nucleic acids and their protein complexes [see Cimino et al. (1985) for a review]. Consequently, much effort has been devoted to the study of photoreactions between psoralens and DNA both in vitro and in vivo.

It has been found that psoralens mainly photoreact with DNA by [2 + 2] cycloaddition reactions between the 4′,5′-furan bond of the psoralen and the 5,6 bond of the thymine bases. 4′,5′-Furanocytosine and 3,4-pyronothymine adducts are found as minor photoreaction products (Straub et al., 1981; Kanne et al., 1982a). DNA interstrand cross-links are produced when the 3,4 and the 4′,5′ double bonds of the psoralens react with the 5,6 double bonds in adjacent thymines of opposite strands (Kanne et al., 1982b), and recent results with octanucleotides indicate that 5′-TA sites are photo-cross-linked at least 10-fold more efficiently than 3′-TA sites by 4′-(hydroxymethyl)-4,5′,8-trimethylpsoralen (Gamper et al., 1984).

A nick translation assay using *Escherichia coli* DNA polymerase I has previously been used to map 4′-(hydroxymethyl)-4,5′,8-trimethylpsoralen adducts in ϕX174 phage DNA (Piette & Hearst, 1983). However, this assay can only be employed if DNA containing a site-specific single-strand nick is at hand. Methods for determining psoralen cross-linking sites in RNA have also been developed by using either reverse transcriptase (Youvan & Hearst, 1982) or mung bean nuclease (Hui & Cantor, 1985). Furthermore, the *E. coli* ABC excinuclease may be used to locate psoralen monoadducts in DNA (Sancar et al., 1985).

In the present report, we describe a new, generally applicable enzymatic method for the determination of psoralen photo-cross-linking sites in DNA at the nucleotide level. This is based on digestion of double-stranded DNA by the exonuclease *Bal*31 which is found to be arrested at psoralen–DNA interstrand cross-linked sites. Our results show that 5′-TA sequences in high molecular weight linear or supercoiled circular plasmid DNA (pUC19 or pBR322) are highly preferred over 3′-TA sequences for photo-cross-linking with 8-methoxypsoralen or 4,5′,8-trimethylpsoralen. The results also indicate that neighboring base sequences have a strong influence on the susceptibility of the 5′-TA site for photo-cross-linking by psoralens.

Materials and Methods

4,5′,8-Trimethylpsoralen was synthesized according to Bender et al. (1979) in our laboratory by Dr. Gunnar Karup, and 8-methoxypsoralen was from Fluka. Nuclease *Bal*31, DNA polymerase (large fragment), and all restriction enzymes were from Boehringer Mannheim. [α-^{32}P]dATP (3000 Ci/mmol) was from Amersham. The plasmids pUC19 and pBR322 were isolated from *E. coli* JM 103 by standard procedures (Maniatis et al., 1982).

Protocol for Cross-Link Analysis by Bal31 Digestion. The experiments were typically performed as follows, exemplified by the use of pBR322 and 4,5′,8-trimethylpsoralen: Ten micrograms of *Bam*HI linearized pBR322 was purified by phenol extraction and ethanol precipitation and redissolved in 100 μL of 10 mM tris(hydroxymethyl)aminomethane hydrochloride (Tris-HCl), pH 7.5, and 1 mM ethylenediaminetetraacetic acid (EDTA). 4,5′,8-Trimethylpsoralen (0.1–1 μg) was added, and the mixture was irradiated from above in Eppendorf tubes for 60 min with light from a Philips TL 20 W/09 fluorescent light tube (365 nm, 13 J m^{-2} s^{-1}). After irradiation, the DNA was precipitated with ethanol. An aliquot of this cross-linked DNA (1 μg) was redissolved in 10 μL of 2 mM Tris-HCl, pH 7.2, 60 mM NaCl, 12.5 mM $MgCl_2$, 12.5 mM $CaCl_2$, and 0.1 mM EDTA and treated with 0.15 unit of *Bal*31 for 0–5 min at 30 °C. The reactions were stopped by adding 1 μL of 0.5 M EDTA. The *Bal*31 treatment removed 300 base pairs (bp) per minute initially. Subsequently, the DNA was purified by phenol extraction after addition of 20 μg of carrier tRNA, treated with 1 unit of restriction enzyme *Hin*dIII for 2 h at 37 °C, once again purified by phenol extraction, and redissolved in 10 μL of H_2O. Radioactive labeling was performed with 5 μL of this solution to which was added 5 μL of H_2O, 1 μL of concentrated buffer (0.5 M Tris-HCl, pH 7.2, 0.1 M $MgSO_4$, 1 mM dithiothreitol, and 0.5 mg/mL bovine serum albumin), 2 μCi of [α-^{32}P]-dATP, and 0.5 unit of *E. coli* DNA polymerase (large fragment). The mixture was incubated at 37 °C for 45 min, and 50 μL of 0.2 M sodium acetate in ethanol was added (−20 °C, 1 h). The DNA was pelleted, washed with ethanol, dried, redissolved in 10 μL of TBE buffer (90 mM Tris–borate, pH 8.3, and 10 mM EDTA) and 20% glycerol, and analyzed by electrophoresis on 10% polyacrylamide [0.3% bis(acrylamide)] gels.

Results

Psoralen Photo-Cross-Linking Sites in the EcoRI–HindIII Fragment of pUC19. *Bal*31 possesses a double-strand-specific exonuclease activity, and we assumed that a psoralen–DNA interstrand cross-link would be a severe obstacle for the enzyme. Therefore, we expected that exhaustive *Bal*31 digestion of psoralen-cross-linked double-stranded specific DNA fragment would result in the generation of a series of DNA molecules with cross-links in both ends (Figure 1). Subsequent cleavage with a restriction enzyme which only cleaves once within the DNA molecule and end labeling of the restriction site would thus create labeled DNA fragments extending from the restriction site to a psoralen cross-linking site. Consequently, the cross-linking sites could be determined on the basis of the length of these fragments. Furthermore, if the restriction site is asymmetrically located on the original DNA fragment, two size classes of fragments originating from either end of the original DNA molecule would be produced provided that the cross-linking degree of the large fragment is $\gg 1$. Alternatively, nonexhaustive *Bal*31 digestion can be employed if the conditions are optimized for complete digestion of the small fragment (cf. Figure 1).

We tested this protocol using the plasmid pUC19 (Figure 2) which was linearized with *Eco*RI and treated with 4,5′,8-trimethylpsoralen (TMP) and long-wavelength ultraviolet light. A fraction of this cross-linked DNA was 3′ labeled with ^{32}P, cleaved with *Hin*dIII, heat denatured, and analyzed by polyacrylamide gel electrophoresis (Figure 3). From these results, it may be estimated that 1 μg/mL TMP produced one cross-link per 150 bp (lane 2) while 10 μg/mL TMP produced one cross-link per 80 bp (lane 3). Analogous treatment of supercoiled pUC19 plasmid resulted in cross-linking ratios of 1/100 and 1/60 (Figure 3, lanes 4 and 5). The more efficient cross-linking of supercoiled DNA is attributed to an increased binding affinity for the psoralen. It is well-known that intercalators in general have higher affinity for supercoiled DNA (Gale et al., 1981). *Eco*RI-linearized pUC19 DNA which contained one cross-link per 150 bp was used for the *Bal*31 digestion experiments. Following *Bal*31 digestion, the DNA was cleaved with *Hin*dIII (Figure 2), 3′ end labeled, and analyzed by polyacrylamide gel electrophoresis. The results, which are presented in Figure 4, show that three major small fragments of approximate sizes 51 bp (undigested *Eco*RI–*Hin*dIII fragment), 41 bp (*Bal*31 stop at position 409), and 26 bp (*Bal*31 stop at position 424) are produced. Similar

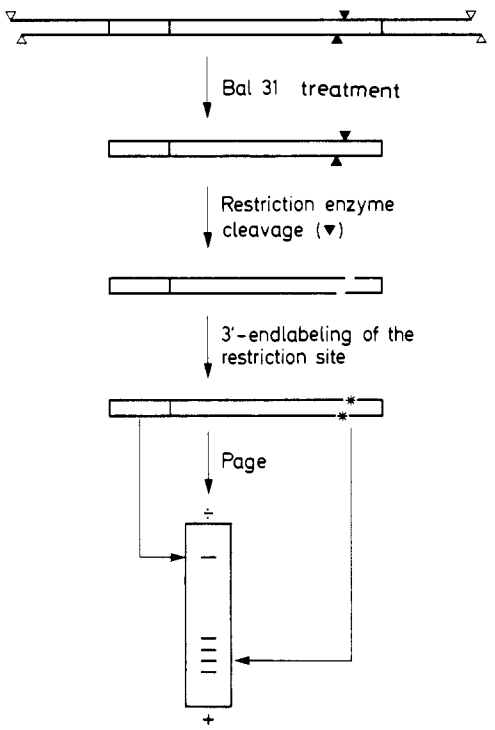

FIGURE 1: Schematic outline of the procedure for psoralen cross-link analysis using exonuclease *Bal*31. Treatment of the cross-linked DNA in question with the first restriction enzyme [(▽) cf. Figure 2] produces a linear double-stranded DNA fragment which is treated with *Bal*31. Asymmetric cleavage by the second restriction enzyme [(▼) cf. Figure 2] results in a class of short fragments and a class of longer fragments, which all terminate at a psoralen cross-link and which can be labeled with ^{32}P at the restriction site. Analysis by polyacrylamide gel electrophoresis (Page) will separate DNA fragments (small class) extending from the restriction site (▼) to a psoralen interstrand cross-link while the class of larger fragments will not be separated at the top of the gel. If the original DNA restriction fragment (▽) on the average contains less than one cross-link, the analysis can still be performed by optimizing the *Bal*31 digestion to remove a number of base pairs corresponding to the short distance between the restriction sites (▼, ▽).

treatment of untreated DNA, which did not contain any psoralen–DNA interstrand cross-links, only gave rise to labeled fragments at shorter digestion times, indicating a temporary arrest of the enzyme action at these sites (Figure 4, lanes 1–3). Therefore, we conclude that psoralen–DNA interstrand cross-links inhibit the exonuclease activity of *Bal*31. Moreover, we infer that the enzyme is arrested only a few base pairs, if not directly, in front of a cross-link, since the stops oocur at two 5′-TA sites, namely, T_{410} and T_{425}. The cross-linking at T_{410} was furthermore indicated by the resistance of the cross-linked DNA to cleavage with restriction enzyme *Kpn*I (Zhen et al., 1986). Thus, we observed that photo-cross-linking of pUC19 in the 401–447 region takes place at the 5′-TA sites, T_{410} and T_{425}, whereas no cross-linking of the 3′-TA sites, A_{419} and A_{443}, was detected. It should be noted that indistinguishable results were obtained with supercoiled DNA and that similar experiments using 8-methoxypsoralen instead of TMP also resulted in cross-linking only at 5′-T_{410}A and 5′-T_{425}A (data not shown).

Photo-cross-linking sites in the 346 bp BamHI–HindIII fragment of pBR322 (Figure 2a) were determined by a procedure analogous to the one described for pUC19. The results are presented in Figures 2a, 5, and 6. Due to the length of this fragment combined with the influence of the cross-link on the migration of the DNA (which is believed to be slight since the cross-link is positioned at the end of the DNA), only approximate determinations of the *Bal*31 stops can be obtained as indicated in Figure 2a. However, also in this case it is evident that all bands in the gel may be assigned to fragments in which *Bal*31 has stopped in front of a 5′-TA site. The difference between 5′-TA and 3′-TA sites is less clear in this case since the resolution is insufficient to distinguish between adjacent 5′-TA/3′-TA sites which are very abundant in this DNA fragment. However, the majority (~80%) of the non-cross-linked TA sites appear to be 3′-TA.

It is interesting that some 5′-TA sites, e.g., 5′-T_{94}A and 5′-T_{324}A, do not appear to give rise to significant *Bal*31 fragments (Figure 5). It should be noted that the results presented in Figure 5, lanes 9 and 10 were obtained at a cross-linking ratio of less than one per fragment. At higher cross-linking ratios, the intensities of the smaller fragments decreased relative to those of the large fragments (Figure 5, lanes 6 and 7 vs. lanes 9 and 10), indicating that *Bal*31 exonuclease is effectively stopped by the first cross-linked site encountered.

Although we do not have any direct proof that *Bal*31 is stopped only at cross-links and not at monoadducts, too, we feel safe to draw this conclusion based on the following arguments: First, all of the observed *Bal*31 arrests can be assigned to a potential 5′-TA cross-linking site, and second, all labeled *Bal*31 fragments are readily renaturable, indicating that they all contain an interstrand cross-link (Figure 6) even though the original DNA fragments prior to *Bal*31 digestion contained less than one cross-link per fragment.

DISCUSSION

By analyzing the psoralen photo-cross-linking of the *Eco*RI–*Hin*dIII fragment of the pUC19 plasmid, we found two major cross-linked sites, namely, 5′-TA_{411}, and 5′-TA_{426}, while we did not detect any cross-linking of the sites 5′-AT_{420} and 5′-AT_{444}. This is in accordance with the report that the oligonucleotide 5′-CGGTACCG is photo-cross-linked at least 10 times more efficiently by 4′-(hydroxymethyl)-4,5′,8-trimethylpsoralen than is 5′-CGGATCCG (Gamper et al., 1984).

The apparent preference for photo-cross-linking of 5′-TA sequences is somewhat in conflict with the results of Kanne et al. (1982b), who concluded that both diastereoisomers of the *cis-syn*-dT–psoralen–dT adduct were present in the reaction products of DNA with either 8-methoxypsoralen or 4,5′,8-trimethylpsoralen (in 7/4 and 1/1 ratios, respectively). Their results therefore strongly indicate that diadducts are formed at both 5′-TA and 3′-TA sequences. However, these authors used much higher psoralen to base pair ratios which led to one cross-link per 50 base pairs (8-methoxypsoralen) or to one per 23 base pairs (4,5′-8-trimethylpsoralen) whereas our experiments were carried out at cross-linking ratios of 1/150 (pUC19) or 1/900 (pBR322). Thus, there appears to exist a preference but not an exclusivity for psoralen cross-linking of 5′-TA sequences.

The observed preference for cross-linking at 5′-TA sequences corresponds well with molecular model building. By using the base pitch angles obtained by X-ray crystallography (Dickerson & Drew, 1981; Dickerson, 1983), and taking the unwinding angle of the psoralen into account (28°; Wiesehahn & Hearst, 1978), it is clearly seen that the 5′-TA sequence is considerably better oriented for T–psoralen–T cross-linking than the 3′-TA (Figure 7), which must require that the involved double bonds are approximately parallel. This may be a naive argument considering that two consecutive photoreactions are required and that it is the configuration of the intercalated psoralen in the excited state which is involved in the photoreaction. However, we find the correlation striking. Furthermore, the quantum yield of the secondary photo-

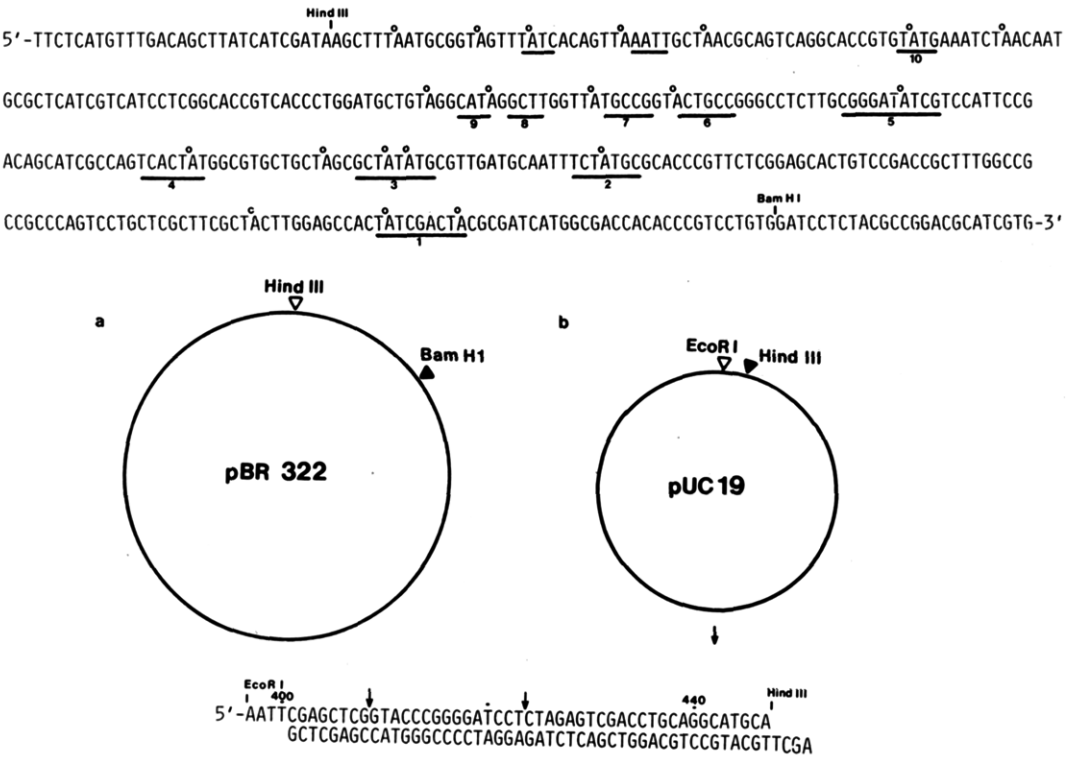

FIGURE 2: (a) Position of the *Hind*III and *Bam*HI restriction sites in the plasmid pBR322 and the sequence of this part of the plasmid (T_1–G_{400}). The positions of the 5′-TA sites (O) are also indicated as are the positions which are detected as psoralen photo-cross-linking sites by the *Bal*31 procedure (cf. Figures 5 and 6): Underlined sequences denote sites of *Bal*31 stop within the uncertainty of the determination. (b) Position of the *Eco*RI and *Hind*III restriction sites in the plasmid pUC19 and the sequence of this part of the plasmid. The sites of *Bal*31 stop (↓) are also shown.

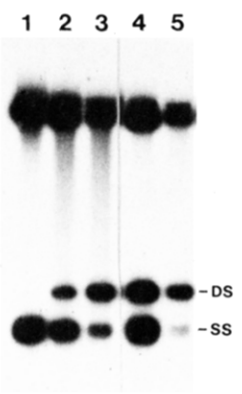

FIGURE 3: Photo-cross-linking of pUC19 with various amounts of 4,5′,8-trimethylpsoralen. Linearized (*Eco*RI) pUC19 (lanes 1–3) or supercoiled pUC19 (lanes 4 and 5) (1 μg) was irradiated in the absence of psoralen (lane 1) or with 0.001 μg/μL (lanes 2 and 4) or 0.01 μg/μL (lanes 3 and 5) 4,5′,8-trimethylpsoralen. Subsequently, the DNA was cleaved with *Hind*III (and *Eco*RI in lanes 4 and 5) and labeled with [α-^{32}P]dATP at the *Eco*RI site. Following heat denaturation, the samples were analyzed on a 10% polyacrylamide gel. DS, double-stranded (i.e., cross-linked) *Eco*RI–*Hind*III fragment. SS, single-stranded (i.e., non-cross-linked) *Eco*RI–*Hind*III fragment.

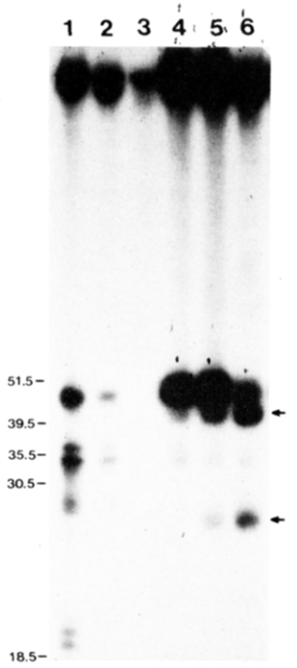

FIGURE 4: Analysis of psoralen cross-linking sites in the *Eco*RI–*Hind*III fragment of pUC19. *Eco*RI-linearized pUC19 was photoreacted with 4,5′,8-trimethylpsoralen, treated with *Bal*31 for 1 (lanes 1 and 4), 4 (lanes 2 and 5), or 10 min (lanes 3 and 6), cleaved with *Hind*III, 3′-^{32}P end labeled, and analyzed by polyacrylamide gel electrophoresis. Lanes 1–3, control DNA; lanes 4–6, psoralen cross-linked DNA. Restriction fragments of pUC19, extending from the *Hind*III site, were used as size markers which are indicated in base pairs. The arrows indicate the DNA fragments containing psoralen cross-links at positions T_{425} and T_{410}, respectively.

reaction is 4 times higher than that of the primary photoreaction, thus favoring this step in the cross-linking (Tessman et al., 1985).

It is also interesing to note that the base tilt angles obtained from X-ray crystallographic studies (Dickerson & Drew, 1981; Dickerson, 1983) show that 5′-TA base pairs are opened ~8° toward the minor groove, while 3′-TA sequences are opened ~8° toward the major groove. Since psoralen intercalation leading to the proper orientation for photocycloaddition is believed to take place with the psoralen hydrophobic edge

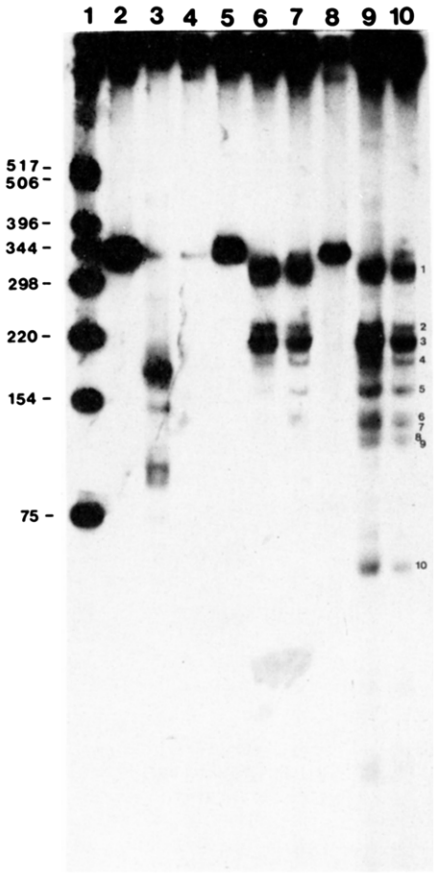

FIGURE 5: Analysis of psoralen cross-linking sites in the *Hin*dIII–*Bam*HI fragment of pBR322. *Bam*HI-linearized pBR322 was photoreacted with 4,5′,8-trimethylpsoralen, treated with *Bal*31 for 0 (lanes 2, 5, and 8), 1 (lanes 3, 6, and 9), or 3 min (lanes 4, 7, and 10), cleaved with *Hin*dIII, end labeled with [α-^{32}P]dATP, and analyzed by polyacrylamide gel electrophoresis. Lane 1, size marker (pBR322 × *Hae*III). Lanes 2–4, non-cross-linked control DNA. Lanes 5–7, DNA containing >1 cross-link per *Bam*HI–*Hin*dIII fragment. Lanes 8–10; DNA containing 0.3 cross-link per *Bam*HI–*Hin*dIII fragment. The numbers in lane 10 refer to the major sites of *Bal*31 stop. This numbering is also used in Figures 2 and 6.

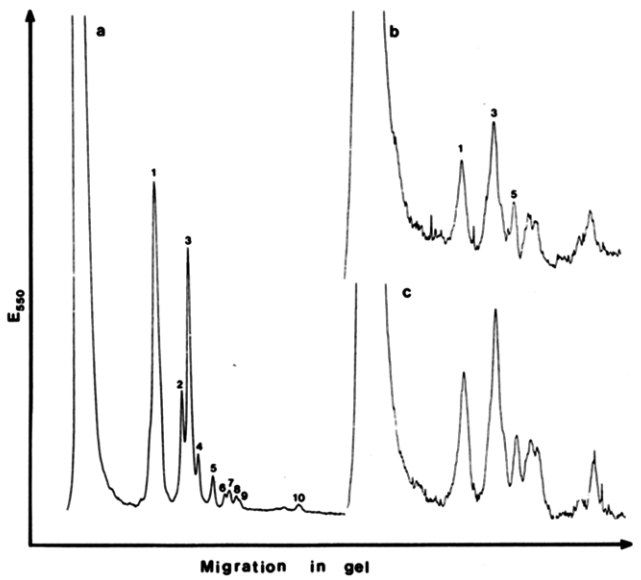

FIGURE 6: Densitometric scans of autoradiograms from an experiment analogous to that described in Figure 5. (a) corresponds to lane 10 of Figure 5 but was obtained from a separate experiment (numbering as in Figures 2 and 5). (b) and (c) were obtained from yet another experiment similar to (a) and were treated identically except that sample b was heat denatured (5 min, 100 °C) prior to being loaded on the gel.

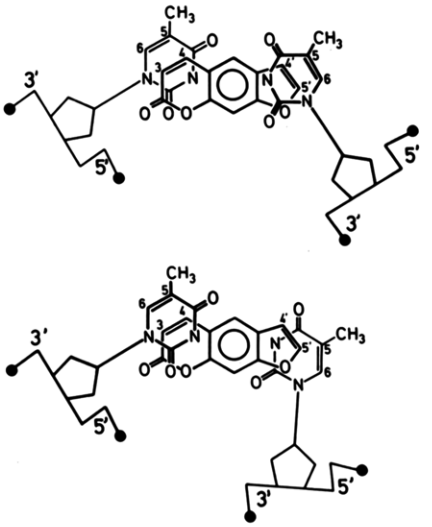

FIGURE 7: Model building showing a psoralen molecule which is intercalated at a 5′-TA (upper) or a 3′-TA (lower) site. Only the thymines of the TA base pairs are shown. If an unwinding angle is not taken into account, the angle between the 5,6-thymine double bond and the 4′,5′-psoralen double bond would be 28° wider, which would still give the 5′-TA sequence the better orientation for cross-linking.

entering from the minor groove (Hansen et al., 1983; Wirth et al., 1986), intercalation at 5′-TA sites should be favored over intercalation at 3′-TA sites.

The analysis of photo-cross-linking sites in the pBR322 plasmid (Figures 2, 5, and 6) indicates that base sequences surrounding the 5′-TA base pair have a significant impact on the cross-linking efficiency. Only ~70% of a total of 20 5′-TA sequences within the analyzed DNA fragment appear to constitute efficient photo-cross-linking sites. The influence of more distant bases on the configuration of the TA base pair in terms of both base pair twist and tilt angle may to some degree be responsible for the variations in photo-cross-linking efficiency at different 5′-TA sites. The possible effect of the neighboring bases on the electronic properties of the thymine, and thereby on the photoreactivity, as well as on the rate of formation and stability of the intercalation complex, i.e., the binding affinity of the psoralen to the individual sites, should also be considered.

The present results do not suggest any obvious three- or four-nucleotide consensus sequence for efficient psoralen cross-linking, but they do indicate that the microheterogeneity of the DNA helix, as reflected in the local conformation of a 5′-TA base pair, may be rather profoundly influenced by more distant bases. The microheterogeneity of the DNA helix is also likely to be influenced by proteins, such as histones, transcription factors, etc., which bind to the DNA. Therefore, it is possible that the psoralens may be used as probes for a detailed study of the chromatin structure, e.g., in relation to transcription. We are currently exploring this aspect of the technique.

Registry No. 8-MOP, 298-81-7; 4,5′,8-trimethylpsoralen, 3902-71-4; exonuclease *Bal*31, 85340-94-9.

REFERENCES

Anderson, T. F., & Voorhees, J. J. (1980) *Annu. Rev. Pharmacol. Toxicol. 20*, 235–257.

Bender, D. R., Hearst, J. E., & Rapoport, H. (1979) *J. Org. Chem. 44*, 2177.

Ben-Hur, E., & Song, P.-S. (1984) *Adv. Radiat. Biol. 11*, 131–171.

Birnboim, H. C., & Doly, J. (1979) *Nucleic Acids Res. 7*, 1513–1523.

Cimino, G. D., Gamper, H. B., Isaacs, S. T., & Hearst, J. E. (1985) *Annu. Rev. Biochem. 54*, 1151–1193.
Dickerson, R. E., & Drew, H. R. (1978) *Proc. Natl. Acad. Sci. U.S.A. 78*, 7318–7322.
Dickerson, R. E., & Drew, H. R. (1981) *J. Mol. Biol. 149*, 761–786.
Gale, E. F., Lundliffe, E., Reynolds, P. E., Richmond, M. H., & Waring, M. J. (1981) *The Molecular Basis of Antibiotic Action*, pp 258–401, Wiley, London.
Gamper, H., Piette, J., & Hearst, J. E. (1984) *Photochem. Photobiol. 40*, 29–34.
Hansen, J. B., Bjerring, P., Buchardt, O., Ebbesen, P., Kanstrup, A., Knudsen, P. H., Nielsen, P. E., Norden, B., & Ygge, B. (1985) *J. Med. Chem. 28*, 1001–1010.
Hui, C.-F., & Cantor, C. R. (1985) *Proc. Natl. Acad. Sci. U.S.A. 82*, 1381–1385.
Kanne, D., Straub, K., Rapoport, H., & Hearst, J. E. (1982a) *Biochemistry 21*, 861–871.
Kanne, D., Straub, K., Hearst, J. E., & Rapoport, H. (1982b) *J. Am. Chem. Soc. 104*, 6754–6764.
Maniatis, T., Fritsch, E. F., & Sambrook, J. (1982) *Molecular Cloning, a Laboratory Manual*, Cold Spring Harbor Laboratory Press, Cold Spring Harbor, NY.
Piette, J. G., & Hearst, J. E. (1983) *Proc. Natl. Acad. Sci. U.S.A. 80*, 5540–5544.
Sancar, A., Franklin, K. A., & Sancar, G. (1985) *J. Mol. Biol. 184*, 725–734.
Straub, K., Kanne, D., Hearst, J. E., & Rapoport, H. (1981) *J. Am. Chem. Soc. 103*, 2347–2355.
Tessman, J. W., Isaacs, S. T., & Hearst, J. E. (1985) *Biochemistry 24*, 1669–1676.
Wiesehahn, G., & Hearst, J. E. (1978) *Proc. Natl. Acad. Sci. U.S.A. 75*, 2702–2707.
Wirth, M., Ygge, B., Nielsen, P. E., Buchardt, O., & Norden, B. (1986) *Photochem. Photobiol.* (in press).
Youvan, D. C., & Hearst, J. E. (1982) *Anal. Biochem. 119*, 86–89.
Zhen, W.-P., Jeppesen, C., & Nielsen, P. E. (1986) *Photochem. Photobiol. 44*, 47–51.

Free Energy of Hydrolysis of Tyrosyl Adenylate and Its Binding to Wild-Type and Engineered Mutant Tyrosyl-tRNA Synthetases†

Tim N. C. Wells, Calvin K. Ho,‡ and Alan R. Fersht*
Department of Chemistry, Imperial College of Science and Technology, London, SW7 2AY, U.K.
Received April 4, 1986; Revised Manuscript Received June 2, 1986

ABSTRACT: The equilibrium constant for the formation of tyrosyl adenylate and pyrophosphate from ATP and tyrosine in solution has been measured by applying the Haldane relationship to wild-type and three mutant tyrosyl-tRNA synthetases from *Bacillus stearothermophilus*. The formation constant (=[Tyr-AMP][PP_i]/[ATP][Tyr]) at pH 7.78, 25 °C, and 10 mM $MgCl_2$ is $(3.5 \pm 0.5) \times 10^{-7}$. This corresponds to a free energy of hydrolysis of tyrosyl adenylate at pH 7.0 and 25 °C of −16.7 kcal mol^{-1}. All necessary rate constants had been determined previously for the calculations apart from the dissociation constant of tyrosyl adenylate from its enzyme-bound complex. This was measured by taking advantage of the 100-fold difference in hydrolysis rates of the tyrosyl adenylate when sequestered by the enzyme and when free in solution. These are technically difficult measurements because the dissociation constants are so low and the complexes unstable. The task was simplified by using mutants prepared by site-directed mutagenesis. These were designed to have different rate and equilibrium constants for dissociation of tyrosyl adenylate from the enzyme-bound complexes. The dissociation constants were in the range $(3.5–38) \times 10^{-12}$ M, with that for wild type at 13×10^{-12} M. The four enzymes all gave consistent data for the formation constant of tyrosyl adenylate in solution. This not only improves the reliability of the measurement but also provides confirmation of the reliability of the measured kinetic constants for the series of enzymes.

Aminoacyl adenylates are key intermediates in protein biosynthesis. Despite this importance, their free energies of formation and hydrolysis are unknown. The group transfer potentials of aminoacyl adenylates are expected to be high since they are mixed acid anhydrides (Jencks, 1957): the free energy of hydrolysis of luciferyl adenylate is −13.1 kcal mol^{-1} (Rhodes & McElroy, 1958), and the free energy of hydrolysis of acetyl adenylate is at least −13.3 kcal mol^{-1} (Jencks, 1957). It has become important for us in our studies of the tyrosyl-tRNA synthetase from *Bacillus stearothermophilus* (Figure 1) to know the free energy of formation of tyrosyl adenylate from ATP and pyrophosphate. In these studies, we have measured for Figure 1 the dissociation constants of tyrosine (K_t), ATP (K'_a), and pyrophosphate (K_{pp}) and the rate constants k_3 and k_{-3} for the formation of enzyme-bound tyrosyl adenylate and its pyrophosphorolysis for wild-type and a series of mutant tyrosyl-tRNA synthetases (Wells & Fersht, 1986; Ho & Fersht, 1986). Clearly, if we can measure the dissociation constant of tyrosyl adenylate (K_{ta}) from the enzyme–tyrosyl adenylate complex then we can calculate the equilibrium constant (K_{eq}) for the formation of tyrosyl adenylate and pyrophosphate from tyrosine and ATP from a simple ther-

† This work was funded by the MRC of the U.K.
‡ Present address: Department of Chemistry and Chemical Engineering, California Institute of Technology, Pasadena, CA 91125.

0006-2960/86/0425-6603$01.50/0